Ultrafast laser-induced microexplosions in transparent materials

Eli N. Glezer, Li Huang, Rich J. Finlay, Tsing-Hua Her, J. Paul Callan, Chris Schaffer and Eric Mazur
Division of Engineering and Applied Sciences, and Department of Physics
Harvard University, Cambridge, MA 02138

ABSTRACT

Submicron-diameter structures can be produced inside many transparent materials by tightly focused 100-fs laser pulses. The ultrafast energy deposition creates very high temperature and pressure inside the region, initiating a 'microexplosion'. Material is ejected from the center and forced into the surrounding volume, forming a void surrounded by densified material. Scanning electron microscopy and atomic force microscopy show structural changes confined to an area 200 nm in diameter.

Keywords: microexplosion, nonlinear absorption, laser damage, transparent materials, ultrafast phenomena, ultrashort laser pulses, voxels, ablation, materials processing, optical data storage.

1. INTRODUCTION AND BACKGROUND

We have recently discovered that submicron-diameter structures can be produced inside many transparent materials by tightly focused ultrashort laser pulses.[1-3] These structures or voxels have a high contrast in index of refraction and can be used for recording bits in multiple planes for high density 3-D optical data storage and other applications that involve writing very fine-scale patterns inside transparent materials.[1-3] In this paper we present the results of optical and structural examination of these submicron-diameter voxels and describe in more detail the physical processes involved in their formation.

1.1. Laser damage in transparent materials: nanosecond pulses

Laser-induced damage in transparent materials has been a common phenomenon since its first observation in 1963, when transparent dielectrics were damaged by a pulsed ruby laser[4]. Damage can occur at the surface or in the bulk of the material. The fluence threshold for damage is always lower at the surface, so for unfocused laser beams damage usually first occurs at the surface. If, on the other hand, the beam is focused inside a transparent material by an external lens or by internal self-focusing, the damage can be confined entirely inside the bulk of the medium. The damaged region produced by focused nanosecond pulses is usually characterized by an irregular shape, extensive cracking, and strong optical scattering. With self-focused nanosecond pulses, long filaments are produced by a focus that moves back (opposite to the direction of light propagation) as the intensity increases during the pulse.[5]

The underlying goal in optical damage experiments has been to understand the cause of the damage so that materials can be perfected to withstand very high intensities. With nanosecond pulses, the damage threshold is usually determined by extrinsic factors such as impurities, crystal imperfections and, in the case of surface damage, by surface imperfections. Wide fluctuations in measured thresholds are typical, and damage is not necessarily initiated at the point of highest intensity.

1.2. Surface ablation: ultrashort vs. nanosecond pulses

Recent experiments using picosecond and sub-picosecond laser pulses for surface ablation of transparent materials have shown that the effect of these pulses on the material is quite different from that of longer pulses.[10-14] Rather than depending on impurities or surface imperfections, the ablated area depends only

SPIE Vol. 2966 • 0277-786X/97/$10.00

on the beam profile. The energy deposition is initiated through a multi-photon absorption process (an intrinsic process), rather than depending on extrinsic effects for creating the initial electrons. Because the energy deposition is deterministic rather than statistical, there is very little shot-to-shot fluctuation in the fluence threshold for ablation.

Once the initial electrons are excited across the bandgap through multi-photon absorption, they acquire excess kinetic energy through sequential linear absorption and then scatter off other electrons exciting them across the bandgap by impact ionization. These new free electrons can then also undergo linear absorption, and this process continues as an avalanche. For pulses shorter than about 30 fs, a theoretical model suggests that multiphoton ionization alone is sufficient to produce the critical density of electrons for ablation.[13] Multiphoton absorption is dominant because of the high intensity, and because less time is available for a collisional avalanche during the sub-30-fs duration of the pulse.

With sub-picosecond pulses, the energy is deposited well before any ablation takes place. Moreover, the electrons are ionized and heated faster than they can transfer their excess energy to the lattice. Thus a hot plasma is formed before the lattice is significantly heated. A comparison can be made to recent experiments on GaAs with 70-fs excitation, where a lattice heating time of about 10 ps has been observed below the damage threshold.[15] Above the threshold, changes in the lattice structure of GaAs are directly driven by the destabilization of the covalent bonding in less than 1 ps. This behavior is in contrast to excitation with pulses longer than a few picoseconds, where the laser pulse continues to deposit energy as the lattice heats up and possibly undergoes structural changes. Observations of the surface of fused silica after laser damage show that the morphology of the ablated surface also depends on the pulse duration: with pulses longer than about 20 ps, the damaged area is characterized by melting and boiling of the surface, whereas with pulses shorter than 10 ps, a shallow crater is produced where a thin layer of material has been removed by ablation.[13]

1.3. Bulk vs. surface

An ultrashort pulse focused *inside* a transparent material deposits energy only in the focal volume, where the intensity is high enough for multiphoton absorption. The basic mechanisms for absorption — multiphoton and avalanche ionization — are the same in the bulk as at the surface. However, while surface states can contribute to absorption at the surface, in the bulk an electron must be excited across the entire energy bandgap (assuming the concentration of impurities is low). Additionally, in the bulk the role of self-focusing[16] needs to be considered, as well the defocusing effect of the plasma produced by the propagating pulse.

After the energy is deposited by the laser pulse, the atomic lattice begins to respond to the electronic excitation, but ablation is not possible because the excited volume is in the bulk of the material. The expansion that normally accompanies heating, melting, and vaporization is restrained by the surrounding lattice which serves as an ideal confinement chamber, possibly producing tremendous pressures especially in extremely hard materials such as sapphire.

2. DESCRIPTION OF EXPERIMENTS

The experiments described in this paper are performed with a Kerr-lens-modelocked, regeneratively amplified Ti:Sapphire laser[17]. Chirped-pulse amplification[18] is used to avoid nonlinear optical effects in the amplifier. The 100-fs pulses from the laser oscillator are stretched to 200 ps, injected into an amplifier cavity, ejected after being amplified to 1 mJ in 25 roundtrips, and then recompressed to about 100 fs. A regenerative amplifier has the advantages of excellent mode quality directly out of the amplifier cavity, and very good pulse-to-pulse energy stability due to strong gain-saturation. After recompression, the

amplified output is a 1-kHz train of 100-fs, 500-μJ pulses centered at a wavelength of 780 nm. Less than 0.1% of the laser pulse energy is needed to drive the microexplosions.

To tightly focus the pulses inside the transparent material we use a 0.65 numerical aperture (NA) microscope objective. Refraction at the surface of the material causes spherical aberration, which adversely affects the focusing at depths greater than about 100 μm. Deeper focusing can be achieved by using either an objective with adjustable spherical aberration, or one that is optimized for focusing to a specific depth together with a compensator plate of variable thickness.

In our 3-D data storage experiments,[1-3] we translate the sample in the transverse plane, and move the focusing objective along the beam axis with numerically controlled translation stages with 0.1-μm precision. The bit pattern is controlled by a mechanical shutter. The multiple 2-D data planes were usually written in the back-to-front-plane order, but writing in the front-to-back order was also tested. No noticeable difference was observed between the two writing modes.

To determine the threshold for observable structural change, we wrote regularly spaced arrays of voxels of decreasing pulse energy, all at the same depth of about 100 μm, and examined the area under a high-power microscope with up to 0.95 NA. Having a regularly spaced array of points made detection near the threshold of visible change much easier. Above the threshold, the voxels are visible either in transmission mode, or in scattered light using off-axis illumination.

Most of the results presented below were obtained in fused silica samples. We also examined the effects of tightly-focused ultrashort pulses in other materials, including several optical glasses, amorphous quartz, optical-grade sapphire, plastics (acrylics), and diamond.

For observation under a scanning electron microscope (SEM) and an atomic force microscope (AFM), we polished the material until the surface level reached the plane of voxels using diamond paste. Final polishing of the fused silica samples was done with Cerium Oxide. For SEM examination, the sample was coated with 30-nm of gold by sputtering.

To compare the effect of ultrafast excitation to the effect of longer laser pulses we used the 200-ps uncompressed output of the Ti:Sapphire amplifier, as well as 10-ns pulses from a Nd:YAG laser. The uncompressed Ti:Sapphire pulses are ideal for examining the effect of longer pulsewidth, because the laser mode, wavelength, and focusing are identical to the 100-fs pulses.

3. RESULTS

Figure 1 shows an example of an array of voxels written in a binary data pattern inside fused silica, using 0.5-μJ, 100-fs, 780-nm pulses focused by a 0.65 numerical aperture (NA) microscope objective. Under these focusing conditions, the threshold for structural change is 0.3 μJ. The spacing between adjacent bits is 2 μm. We recorded 10 layers spaced by 15 μm, using a standard 0.65 NA refractive objective. The image is read out using transmitted light in a microscope with a 0.95 NA objective. The written spots can be viewed as dark or bright points depending on the position of the read-out objective. During read-out, the depth discrimination provided by the short depth-of-field of the 0.95 NA objective is sufficient if adjacent layers are spaced by about 10 μm or more. The longitudinal extent of the structurally altered regions is about 2.5 μm.

With 100-fs pulses small, regularly-shaped voxels are produced by pulses in a wide energy range of up to three times the 0.3-μJ threshold for structural change in fused silica. Both the diameter and the longitudinal extent increase with energy. Pulses of even higher energy produce a head-and-filament structure of 20–40-μm length that is visible to the unaided eye. We observed no cracking with the 100-fs pulses in

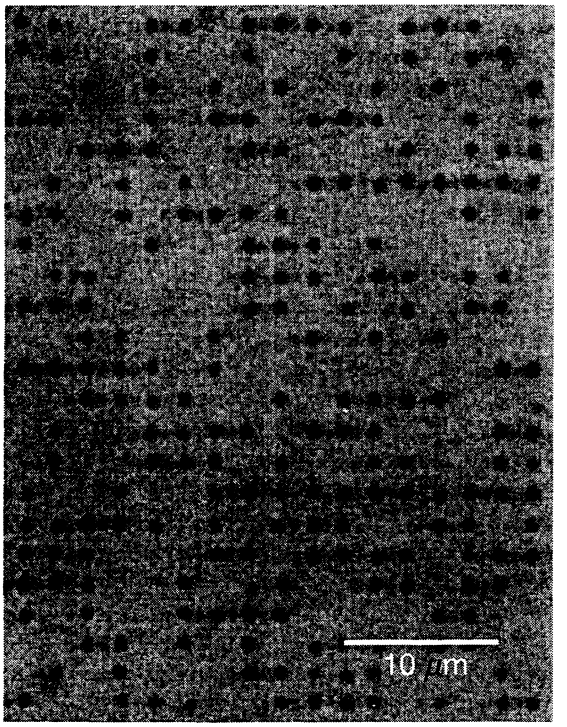

Fig. 1. Binary data pattern stored inside fused silica with 2-μm bit spacing, photographed with an optical microscope using transmitted light.

fused silica even up to pulse energies 100 times the threshold.

We have written arrays of voxels in a wide variety of transparent materials including fused silica, fused quartz, sapphire, BK7 optical glass, and plastic (acrylic). Surprisingly, the threshold for structural change is very similar in all of these materials — within a factor of 2 of the threshold of fused silica. A notable exception is diamond, where the threshold is at least 100 times greater. In all materials, and especially in diamond, the threshold for internal structural change is significantly higher than for surface ablation.

The apparent size of the voxels in Figs. 1 is at the resolution limit of the optical microscope. To obtain information about the extent of the structural changes in the material we polished away the fused silica sample until the surface level reached the internally recorded voxels, and viewed the sample under a scanning electron microscope. Figure 2 shows a SEM image of a 5×5-μm regular array of voxels recorded under conditions identical to those used in the patterns of Fig. 2. The sample is tilted in the SEM to better show the morphology. The bright spots correspond to protrusions or bumps on the surface, while the dark spot (top row second from the right) corresponds to a cavity or pit in the surface. Whether a structurally altered region appears as a bump or a pit depends on the level to which the material is polished. A typical pit is shown at higher magnification in the inset of Fig. 2. Both types of features have diameters of roughly 200 nm.

To examine the morphology of the voxels in more detail, we used an atomic force microscope (AFM). Figure 3 shows examples of depth profiles of the pits and bumps recorded by the AFM. The bumps are 7–10 nm high, while the pits are at least 35–40 nm deep. The pit depth may be greater than the measured

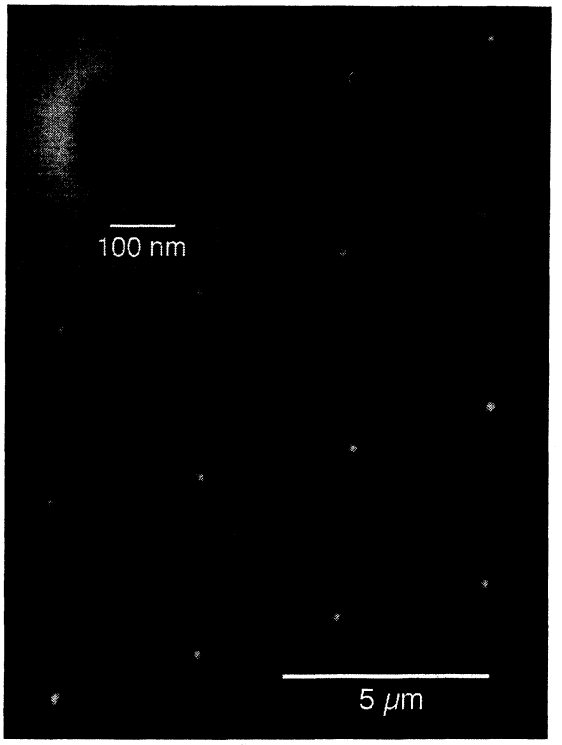

Fig. 2. A tilted SEM view of a polished cross-section through a regular array of voxels with 5-μm spacing. Inset shows a single voxel at higher magnification.

value, because the measurement is limited by the size of the AFM tip (which is pyramidal with a sub-40-nm tip radius). The diameter of both the pits and the bumps is 200–250 nm.

The voxels produced by 100-fs pulses differ drastically from the damaged regions produced by 200-ps and 10-ns pulses. With the longer pulses, the resulting structures are irregularly shaped, and cracks appear in the material even at energies only slightly above the threshold for structural change. An example of the damaged regions produced by 200-ps pulses from the same laser system is shown in Fig. 4. Fig. 4a shows a front view (seen along the direction of the writing beam), and Fig. 4b shows a side view with the laser beam incident from the left. The focusing conditions and beam profile during writing are identical to those used with the 100-fs pulses; the pulse energy is 9 μJ, which is three times the observed threshold with 200-ps pulses; the spacing is 10 μm. Note the large size of the damaged regions, and the clearly visible cracking produced with these longer pulses. The side view shows interesting features in the damaged regions: a drop-shaped front end and an irregularly-shaped and cracked back end.

With 10-ns pulses from a Nd:YAG laser, even larger irregularly shaped damaged regions are produced, and the cracking is more extensive. Figure 5 shows a SEM view of a polished cross-section through a damaged region created inside fused silica by a 10-ns, 30-μJ, 532-nm wavelength pulse focused by a 0.25 NA objective. A cavity appears at the center of the damaged region, surrounded by radiating structural features extending over an area about 20-μm in diameter. Note the dramatic contrast between the SEM views of this highly damaged region and the 200-nm diameter voxels of Fig. 2.

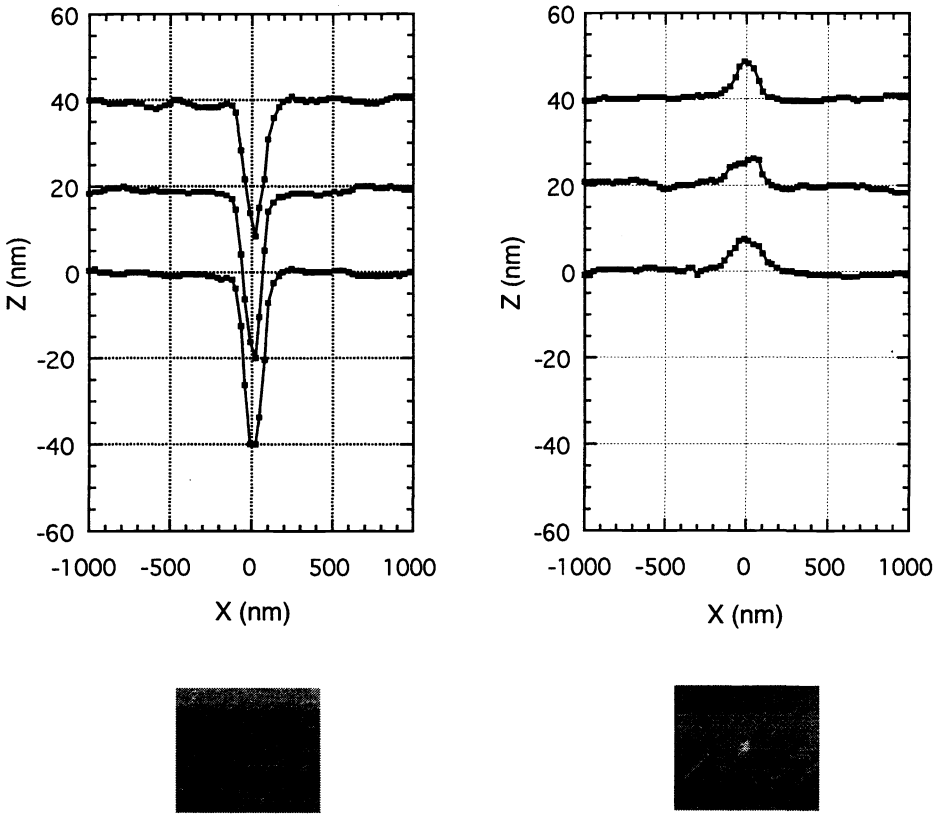

Fig. 3. AFM scans of three pits and three bumps. Also shown are AFM images of a pit and a bump.

4. DISCUSSION

4.1. Size of the voxels

Why are the voxels so small? The FWHM diameter at the focus of our beam is estimated to be 0.9 μm. This assumes that the input beam fills the 0.65 NA objective to the $1/e^2$ intensity point (86% transmission). Any aberrations and imperfections in focusing can only increase the focal area. Yet the optical observations place an upper limit of 0.5-μm on the diameter of the voxels, and the SEM and AFM observations indicate that the diameter of the structurally altered regions is only 200–250 nm.

The submicron diameter is not due to a simple thresholding effect which would occur with an excitation that is only a few percent above the threshold. The 0.5-μJ pulse energy used to make the voxels shown in Figs. 1–3 is well above the observed threshold of 0.3 μJ. Instead, the small size is likely caused by the nonlinearity of the absorption, which creates an excited region significantly smaller than the linear intensity distribution. Furthermore, self-focusing may be reducing the size of the beam waist. Finally, the dynamics of the microexplosion may further confine the extent of the structurally altered region.

The effect of the nonlinearity of the absorption is straightforward. The characteristic diameter of the excited area scales as the inverse of the square root of the order of the nonlinearity. For example, if the absorption is proportional to I^5, then the diameter of the excited volume will be reduced to 45% of the diameter of the intensity distribution.

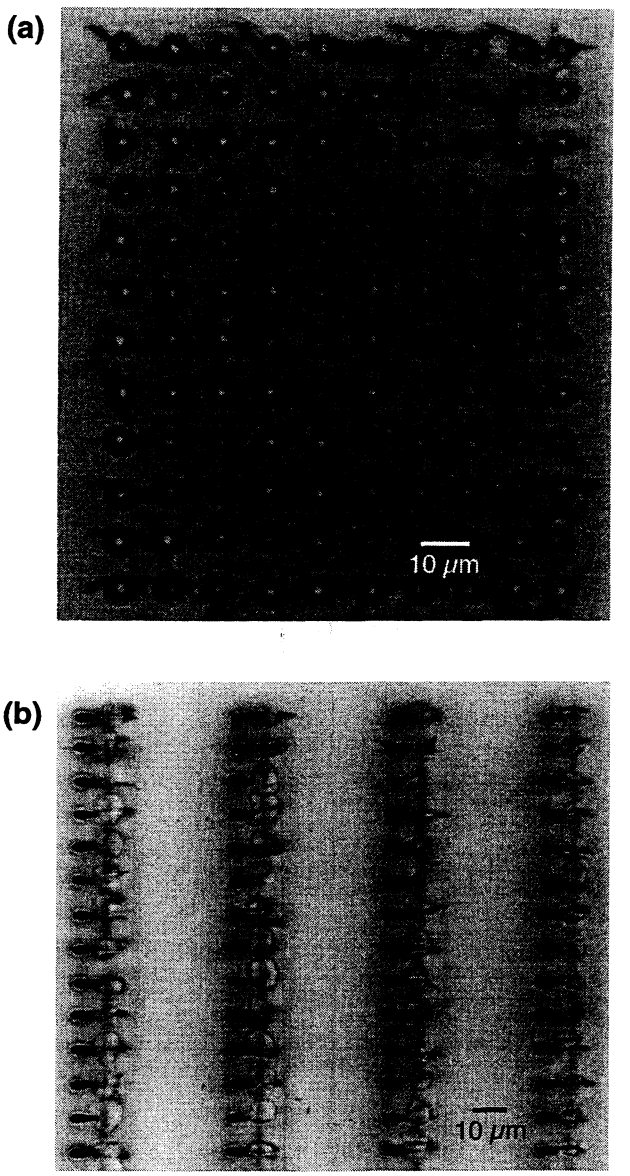

Fig. 4. Damage produced inside fused silica by 200-ps pulses. Optical microscope photograph using transmitted light: (a) front view, (b) side view. Note the differences in scale relative to Fig. 1.

4.2. Self-focusing

The effect of self-focusing is not as easy to predict. One might be expect that under tight external focusing, self-focusing does not play much of a role. However, the intensity in the 100-fs pulses is so high that self-focusing cannot be ruled out. To examine the possible effect of self-focusing on the tightly-focused beam, we model the beam propagation under our experimental focusing conditions, by numerically propagating a Gaussian beam in small steps through the medium. The intensity-dependent focusing is modeled by a progression of lenses of varying strength. Self focusing results from the intensity-dependent radial variation in the index of refraction, $\Delta n = n_2 I$, where n_2 is proportional to the third-order susceptibil-

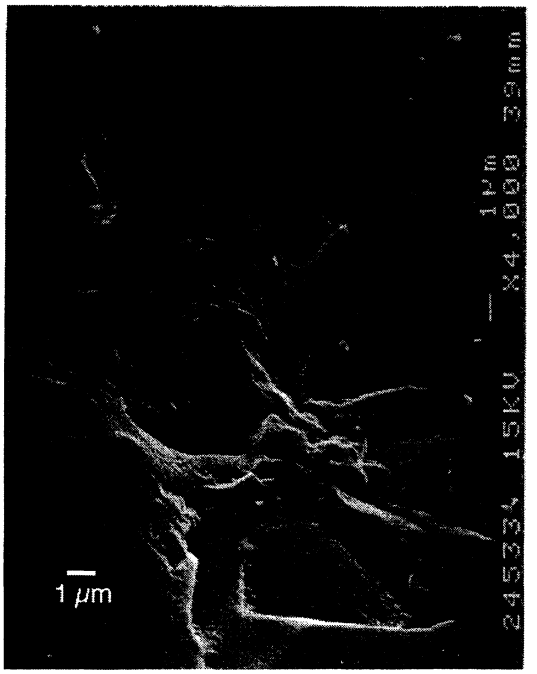

Fig. 5. A SEM view of damage produced inside fused silica by a 10-ns laser pulse.

ity. The strength of the self-focusing lens is proportional to d^{-3}, where d is the beam diameter, because the intensity scales as d^{-2} and the curvature of the phase variation scales as d. We define a parameter s to characterize the strength of the self-focusing,

$$s = (1/\pi)\, n_2 P,$$

P being the power in the beam. With this definition, the effective focal length of the self-focusing lens at any point along the beam is simply

$$f = w^3/s,$$

where w is the $1/e^2$ radius of the beam. Figure 6 shows the beam profile (defined by its $1/e^2$ intensity contour) for varying degrees of self-focusing: $s = 0$, 0.001, 0.0033, and 0.01, expressed in units of μm^2. The beam propagates from left to right. Without self-focusing (dashed curve), the width of the beam waist is $2w_0 = 1.6$ μm, which corresponds to $d_{FWHM} = 0.9$ μm. As the power in the beam is increased, the beam waist moves to the left and its diameter decreases.

Figure 7 shows the beam waist diameter as a function of s. With sufficiently large s, self-focusing significantly reduces the beam waist, even under already tight focusing conditions. For example, at $s = 0.01$ μm^2, d_{FWHM} is reduced to 0.15 μm. To check if this is physically possible we can calculate the maximum Δn that would be produced at the peak intensity. The peak intensity is given by

$$I_0 = (2/\pi)\, (P/w_0^2),$$

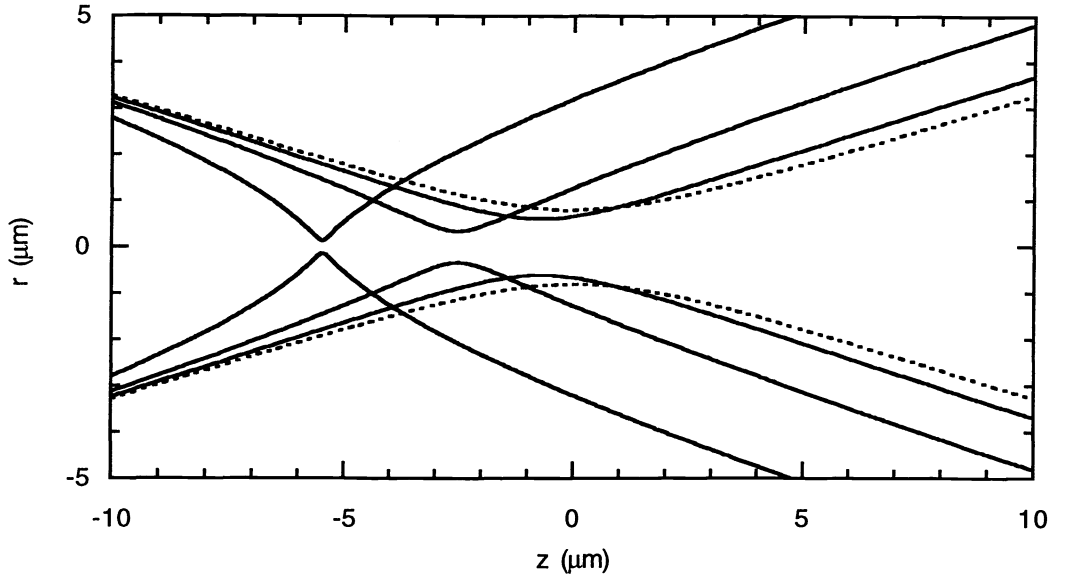

Fig. 6. Effect of self-focusing on the beam profile. Dashed curve: no self-focusing; solid curves: s = 0.001, 0.0033, and 0.01.

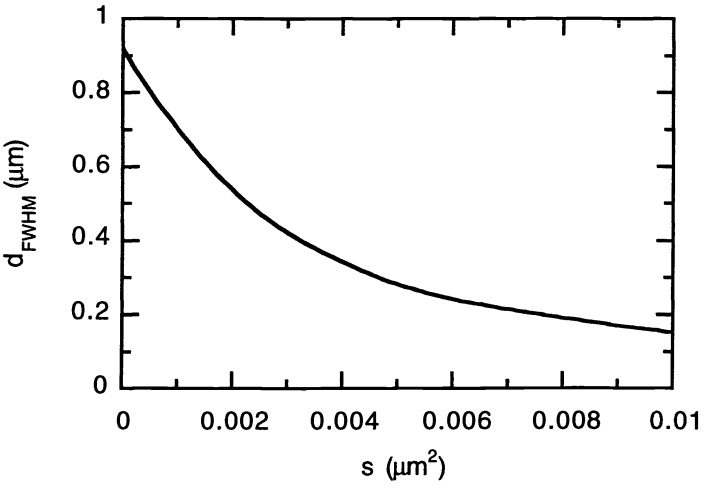

Fig. 7. Beam waist as a function of self-focusing strength.

and the corresponding maximum change in the refractive index is

$$\Delta n_{MAX} = n_2 I_0 = 2\,(s/w_0^2)\,.$$

With $s = 0.01\ \mu m^2$, this results in $\Delta n_{MAX} = 0.9$, a very large change in the refractive index. Several of the approximations in the model are likely to break down before such changes are produced. First, the linear increase of the change in index of refraction with intensity, $\Delta n = n_2 I$, probably saturates and may not be valid at such high intensity. Second, Gaussian beam propagation becomes less accurate in predicting the beam profile under extremely tight focusing. The underlying assumption of the slowly varying

approximation becomes questionable when Δn changes considerably on the scale of a wavelength. Finally, the temporal profile of the pulse needs to be considered, including the effect of self-phase-modulation, which spectrally broadens the pulse. Despite these limitations the model shows that self-focusing can be significant even under tight external focusing conditions when s is large enough.

The magnitude of the self-focusing parameter can be estimated for our experimental conditions. For silica, n_2 is about 3×10^{-16} cm^2/W or 3×10^{-8} μm^2/W. A 100-fs, 0.5-μJ pulse corresponds to a power of 5×10^6 W. Thus, for our experimental conditions s is about 0.05, or 5 times greater than even the largest value considered in Fig. 7. Clearly, self-focusing cannot be ignored.

4.3. Material response

The lattice is heated by the electron plasma on a timescale of 10 ps or less. If the energy of a 0.5-μJ pulse is completely absorbed by a 1-μm^3 volume of fused silica (assuming a 0.75-J/gK heat capacity and 2.2-g/cm^3 density), the silica would be heated to an astounding temperature of 300,000 K. Since the volume remains constant in the confined geometry of the microexplosions, the solid values of the heat capacity are probably valid as rough approximations well above the ordinary melting and boiling temperatures because most of energy ordinarily absorbed in a phase transitions goes into a volume expansion.[22]

The structural observations of the voxels (e.g. Figs. 2 and 3) indicate that a void is formed in the microexplosion, surrounded by densified material. Such a structure could be the result of immense pressure forcing material from the center of the explosion outward. During cooling, the material apparently does not anneal, and the denser phase is frozen in. Further structural analysis is needed to characterize the densified material. Very large pressures are needed to compress materials such as quartz and sapphire. Shock-wave experiments provide information about the compressibility of materials at extremely high pressures.[23,24] For example, in fused quartz, a pressure of 6.1 GPa is needed to produce a 10% volume reduction; a 50% reduction requires 35 GPa.[23] In sapphire, a 37-GPa pressure is needed for a 10% volume reduction (based on parameters measured in Ref.20). Extrapolation of these data suggest that a 50% reduction requires 560 GPa, or over 5 million atmospheres, which is beyond the highest pressures achieved in sapphire shock experiments (340 GPa).[20] The formation of a void surrounded by denser material is particularly intriguing in the case of sapphire, because no transition to a denser phase has ever been seen. Further experiments are needed to determine whether pressures of these magnitudes are indeed produced in the microexplosions.

5. APPLICATIONS

The ultrashort-pulse driven microexplosions described above provide a unique method for writing information inside transparent materials. Information-bearing patterns can be inscribed in the bulk of virtually any transparent solid object. The features that can be inscribed range from precise macroscopic patterns visible to the eye, down to micron and even sub-micron size structures which are only visible under a high-power microscope with proper illumination. With precise 2-axis or 3-axis translation, practically any image can be inscribed, including binary data, alphanumeric characters, identifying codes (visible or covert), and 3-D objects. The size and visibility of each voxel can be controlled by proper choice of focusing conditions and pulse energy.

A potentially significant application of this method is for high-density 3-D data storage, discussed in more detail in other publications.[1–3] By writing multiple 2-D planes of binary data, storage capacities on the order of 1 Tbit should be possible in a standard CD-size format. Special photosensitive materials are not required — ordinary glass or even plastic can be used as the storage medium, a medium that does not need curing or fixing, and is thermally, chemically, and optically stable and inexpensive. The information

is stored permanently, and can only be erased by physically breaking the storage medium, or heating it to the melting or annealing temperature.

The ability to write 3-D objects with sub-micron precision may be useful for creating periodic structures (possibly including photonic bandgap crystals), diffrative optical elements and patterned grating in fibers. The process can also be used for fabricating regions of increased density and hardness in many transparent materials. The range of possible materials is not limited to those transparent to the eye, and includes semiconductors, since the transparency requirement is only that the laser pulse be of lower frequency than the bandgap of the material. The high temperatures and pressures produced in the microexplosions may lead to novel methods for materials processing.

6. CONCLUSION

Nonlinear absorption of a tightly focused ultrashort laser pulse provides a unique mechanism for rapidly depositing energy in a microscopic volume inside a transparent material. Extreme temperatures and pressures are produced inside the material, which results in a microexplosion, forcing material out of the center and into the surrounding volume. In contrast to the large, irregular and cracked damage region produced by nanosecond pulses, the structurally altered region produced by ultrashort pulses is highly localized, regular, and shows no signs of cracking. The internal structures created with ultrashort pulses may find use in such applications as high-density 3-D data storage, sub-surface marking and engraving in transparent objects, fabrication of 3-D optical elements, and materials processing.

7. REFERENCES

1. E. N. Glezer, M. Milosavljevic, L. Huang, R. J. Finlay, T.-H. Her, J. P. Callan, and E. Mazur, to be published in Opt. Lett. **21**, No.24 (1996).
2. E. N. Glezer, M. Milosavljevic, L. Huang, R. J. Finlay, T.-H. Her, J. P. Callan, and E. Mazur, in *Proc. Ultrafast Phenomena* (1996);
3. E. N. Glezer, M. Milosavljevic, L. Huang, R. J. Finlay, T.-H. Her, J. P. Callan, and E. Mazur, OSA Technical Digest, Vol. 12, *International Symposium on Optical Memory and Optical Data Storage,* Maui, Hawaii (1996).
4. P. D. Maker, R. W. Terhune, C. M. Savage, in Proc. 3rd Int. Conf. Quantum Electronics, edited by P. Grivet and N. Bloembergen, (Dunod, Paris 1964).
5. Y. R. Shen, *The Principles of Nonlinear Optics* (John Wiley & Sons, New York, 1984).
6. D. A. Parthenopoulos and P. M. Rentzepis, Science **245**, 843 (1989).
7. J. H. Strickler and W. W. Webb, Opt. Lett. **16**, 1780 (1991); U.S. Patent #5,289,407 (1994).
8. Y. Kawata, H. Ueki, Y. Hashimoto, and S. Kawata, Appl. Opt. **34**, 4105 (1995).
9. H. Ueki, Y. Kawata, and S. Kawata, Appl. Opt. **35**, 2457 (1996).
10. J. Ihlemann, B. Wolff, and P. Simon, Appl. Phys. A **54**, 363 (1992).
11. D. Du, X. Liu, G. Korn, J. Squier, and G. Mourou, Appl. Phys. Lett. **64**, 3071 (1994).
12. B. C. Stuart, M. D. Feit, S. Herman, A. M. Rubenchik, B. W. Shore, and M. D. Perry, Phys. Rev. Lett. **74**, 2248 (1995);
13. B. C. Stuart, M. D. Feit, S. Herman, A. M. Rubenchik, B. W. Shore, and M. D. Perry, J. Opt. Soc. Am. B, **13**, 459 (1996).
14. D. von der Linde and H. Schüler, J. Opt. Soc. Am. B, **13**, 216 (1996).
15. L. Huang, E. N. Glezer, J. P. Callan, and E. Mazur, *Proc. of Quant. Elect. and Laser Science*, Anaheim, CA (1996).
16. M. J. Soileau, W. E. Williams, N. Mansour, Opt. Engineering **28**, 1133, (1989).
17. S. Deliwala, Ph.D. Thesis, Harvard University, 1995.

18. D. Strickland and G. Mourou, Opt. Comm. **56**, 219 (1985).
19. T. Erdogan, OSA Technical Digest, Vol. 11, *Nonlinear Optics: Materials, Fundamentals and Applications*, Mauii, Hawaii (1996).
20. D. Erskine, High-Pressure Science and Technology - 1993, Colorado Springs, CO. AIP Conference Proceedings **309**, 141 (1994).
21. N. W. Ashcroft , N. D. Mermin, *Solid State Physics* (Saunders College, Philadelphia, 1976).
22. R. W. Hopper and D. R. Uhlmann, Journal of Applied Physics **41**, 4023 (1970).
23. *LASL Shock Hugoniot Data*, edited by S. P. Marsh (University of Calif. Press, Berkeley, 1980).
24. I.-Y. S. Lee, J. R. Hill, D. D. Dlott, J. Appl. Phys. **75**, 4975 (1994).